

# Harmonizing Output Imbalance for semantic segmentation on extremely-imbalanced input data

Jianye Yi<sup>1,\*</sup>, Xiaopin Zhong<sup>1,\*</sup>, Weixiang Liu<sup>1,✉</sup>, Zongze Wu<sup>1</sup>, Yuanlong Deng<sup>2</sup>, Zhengguang Wu<sup>3</sup>

<sup>1</sup>Lab. of Machine Vision and Inspection, College of Mechatronics and Control Engineering, Shenzhen University, Shenzhen 518060, China

<sup>2</sup>Shenzhen Institute of Technology, Shenzhen 518116, China

<sup>3</sup>State Key Lab. of Industrial Control Technology, Institute of Cyber-Systems and Control, Zhejiang University, Hangzhou 310027, China

2110296017@email.szu.edu.cn, xzhong@szu.edu.cn, ✉wxliu@szu.edu.cn

zzwu@szu.edu.cn, dengyl@szu.edu.cn, nashwzhg@zju.edu.cn

## Abstract

Semantic segmentation is a high level computer vision task that assigns a label for each pixel of an image. It is challenging to deal with extremely-imbalanced data in which the ratio of target pixels to background pixels is lower than 1:1000. Such severe input imbalance leads to output imbalance for poor model training. This paper considers three issues for extremely-imbalanced data: inspired by the region-based Dice loss, an implicit measure for the output imbalance is proposed, and an adaptive algorithm is designed for guiding the output imbalance hyperparameter selection; then it is generalized to distribution-based loss for dealing with output imbalance; and finally a compound loss with our adaptive hyperparameter selection algorithm can keep the consistency of training and inference for harmonizing the output imbalance. With four popular deep architectures on our private dataset from three different input imbalance scales and three public datasets, extensive experiments demonstrate the competitive/promising performance of the proposed method.

## 1. Introduction

Semantic segmentation is one of the high-level tasks in computer vision, which assigns a label for each pixel of an image, and is able to provide scene understanding at the pixel level [1]. Driven by both academia and industry, the rapid increase of deep learning in semantic segmentation has shown promising performance for real applications, such as in natural images, industrial surfaces, medi-

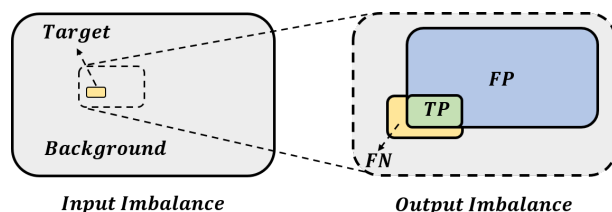


Fig. 1. Input imbalance for training (Left) and output imbalance for inference (Right). The input imbalance refers to the pixel class-imbalance in the input training samples, while the output imbalance refers to the false positive (FP) and false negative (FN) imbalance in the predicted samples.

cal images and autonomous driving [2–7]; just see a recent survey [8] and references therein. However, class imbalance is also encountered in semantic segmentation, which means that there is significant inequality among the number of examples from different classes. One classical example of class imbalance is the foreground-to-background imbalance [9]. Recently, Taghanaki [10] called this imbalance as an *input imbalance* and proposed the concept of *output imbalance*: the input imbalance refers to the pixel class-imbalance in the input training samples, that is, small target pixels are submerged in a large number of background pixels (see Fig.1 Left); while the output imbalance refers to the false positive (FP) and false negative (FN) imbalance between prediction and ground truth (See Fig.1 Right).

In this paper, we consider a case of semantic segmentation on extremely-imbalanced input data. In our solar silicon dataset<sup>1</sup>, the ratio of tiny hidden cracks (THC) pixels to background pixels is 1 : 2228, which is one order of magni-

\*These authors contributed to the work equally and should be regarded as co-first authors.

<sup>1</sup>The dataset is available in <https://github.com/KLIVIS/DIBE/tree/master>

tude lower than that of commonly used public datasets (see data set description in Subsection 4.1). Such severe input imbalance leads to output imbalance for poor generalization. How to deal with such extremely-imbalanced data? This is a challenge.

Generally speaking, the common solutions for class imbalance can be divided into three levels: data, model and loss function respectively [11, 12]. Most of methods focus on loss design, which only cope with the input imbalance. In practice, output imbalance should also be considered in the special applications. For example, Kannan [13] selected binary cross-entropy (BCE) loss to expect a more balanced output of  $FP$  and  $FN$ . Qiu [14] proposed a loss function combining dynamic boundary-insensitive (DBI) Loss and Dice Loss to adjust the output imbalance. Tversky Loss proposed by Salehi et al. [15] applied two hyperparameters to control the weights of false positive and false negative samples in Dice Loss for adjusting the output imbalance. However the output imbalance hyperparameters are empirically pre-defined. It is not clear to measure the output imbalance and guide the parameter setting.

At present, there are also some open problems with imbalanced input and output in semantic segmentation, especially at the output end. The following three issues still exist:

**Lack of both a quantitative measure and a explicit guidance in adaptive hyperparameters selection for output imbalance:** The existing method of measuring output imbalance is similar to that of input imbalance, simply using the ratio of  $FP$  and  $FN$ . This measurement firstly has a large domain in which the ratio is distributed in  $[0, \infty)$ . It is not convenient to observe the changing trend of output imbalance with visualization. Secondly, the influence of true positive (TP) on the output imbalance is not considered. As an important part of the output confusion matrix, it is unreasonable to ignore TPs and only consider FPs and FNs.

**Lack of ability for adjusting output imbalance in distribution-based loss:** The diversity of loss functions is important in the context of machine learning. There are basically two types of loss functions for semantic segmentation, i.e. distribution-based and region-based. There are several region-based loss functions for controlling the output imbalance [15, 16]. In distribution-based loss functions, although Taghanak [10] uses weighted binary cross-entropy (WBCE) Loss to adjust the output imbalance, the class weight is actually used to adapt to the input imbalance. To our knowledge, there is no work on distribution-based loss that can directly adjust the output imbalance. It is even less possible to study the difference between region-based loss and distribution-based loss with regard to the output imbalance.

**Inconsistency between training and inference for**

**extremely-imbalanced input data:** Although there are some various compound losses to improve the model performance [10, 17, 18], they do not realize that a compound loss for improving the performance is the consistency between the training and the inference of one model [19].

To address the above problems resulting from extremely-imbalanced input data, we emphasize that **Data is Imbalanced at Both Ends** (DIBE). Especially, in order to harmonize the output imbalance, this paper proposes (i) a new indicator for measuring the output imbalance and an adaptive output imbalance hyperparameter selection, (ii) a distribution-based loss function with the ability to harmonize the output imbalance, and (iii) a compound loss adapting to the case of extremely-imbalanced input, as follows:

**For the absence of output imbalance indicator,** we propose a so-called output imbalance index ( $OII$ ), which not only considers  $FP$  and  $FN$ , but also takes account of the value of  $TP$  to measure output imbalance. It makes more sense that the output imbalance should be the relationship between the relative values of  $FP$  and  $FN$  regarding  $TP$ . Meanwhile, the most important key of  $OII$  is that it can be used to guide the adaptive selection of output imbalance hyperparameters. Then a guidance algorithm is designed to this end, and we can quickly select the hyperparameters to improve the model performance. Compared with hyperparameters optimization, our guidance greatly reduces the computational complexity and the occupation for computing resources. Please refer to Subsection 3.1 and 4.4 for details.

**For distribution-based loss without adjustment ability of output imbalance,** we propose a distribution-based loss function,  $DIBE_{Dis}$  Loss. By refining the focal loss [20], we divide the hard-to-classify samples into two subgroups: FPs and FNs<sup>2</sup>, and then assign different weights to FPs and FNs in the loss respectively. So it can harmonize the output imbalance with the distribution-based loss. Please refer to Subsection 3.2 and 4.5 for details.

**For inconsistency between training and inference on extremely-imbalanced input data,** we propose a new compound loss function, namely DIBE Loss, combining  $DIBE_{Dis}$  Loss and  $DIBE_{Reg}$  Loss and unifying their hyperparameters (Subsection 3.3, 4.6 and 4.7).  $DIBE_{Dis}$  Loss is the loss function mentioned above, while  $DIBE_{Reg}$  is a region-based loss based on Tversky Loss, which increases the loss gradient of small targets through a simple logarithmic operation and overcomes the loss over-suppression phenomenon of Focal Tversky (FT) Loss when Tversky coefficient ( $Tv$ ) tends to be 1.  $DIBE_{Dis}$  Loss, based on Focal Loss, is better for the hard-to-classify samples optimization. Therefore, it is more suitable for extremely-imbalanced in-

<sup>2</sup>For simplicity,  $FP$ ,  $FN$  and  $TP$  denote the numbers of false positive, false negative and true positive samples, respectively; FPs, FNs and TPs refer to FP, FN and TP samples, respectively.

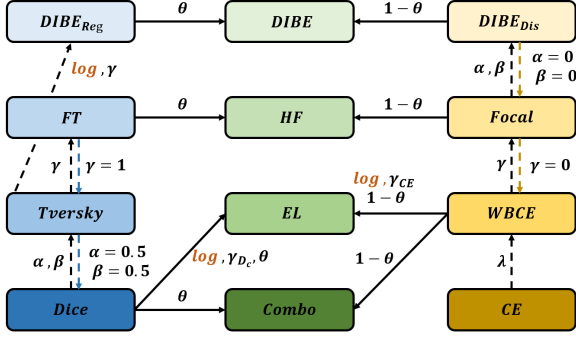


Fig. 2. The similarities and differences between DIBE Loss and typical losses for semantic segmentation. The log stands for the logarithmic operation.  $\theta, \gamma, \lambda, \alpha$  and  $\beta$  represent relevant hyperparameters.

put as  $DIBE_{Reg}$  Loss. And both of them have the ability to harmonising the output imbalance. The similarities and differences between DIBE Loss and the other loss functions mentioned above can be found in Fig. 2.

In summary, we mainly harmonize the imbalance at the output end, and provide the following contributions within the framework of DIBE:

- A novel quantitative index  $OII$  for measuring the output imbalance is proposed, and an adaptive algorithm is also designed. It can explicitly guide the output imbalance hyperparameter adjustment with little computation;
- For the disability of adjusting output imbalance of the existing distribution-based losses, a new distribution-based loss,  $DIBE_{Dis}$  Loss, is generally designed with analogy to region-based loss for harmonizing the output imbalance;
- In order to keep consistency between training and inference on extremely-imbalanced input data, we propose a new compound loss function, DIBE Loss. It combines both region-based and distribution-based losses for harmonizing training and inference.

## 2. Related work

Loss functions in semantic segmentation are crucial. A good loss function can make the network learning more efficient. Ma [21] and Jadon [22] classified the existing segmentation losses into four categories, namely, distribution-based loss, region-based loss, compound loss and boundary-based loss. For each one, there are many classical loss functions. In the following subsections we review their definition, formulation and hyperparameters related to this study.

### 2.1. Distribution-based loss

Cross-entropy [23] is derived from Kullback-Leibler divergence and used to measure the similarity of two distributions for a given random variable or set of events. It is often used for classification and works well in segmentation task. Binary Cross-Entropy (BCE) Loss is an essential distribution-based loss function for segmentation, and widely used because of its effectiveness. For each pixel of image, BCE Loss is defined as:

$$\mathcal{L}_{BCE} = \begin{cases} -\log(\hat{p}), & y = 1 \\ -\log(1 - \hat{p}), & y = 0 \end{cases}, \quad (1)$$

where  $y$  denotes the ground truth of pixel sample, and  $\hat{p}$  is the predicted probability.

Pihur et al. [24] reported Weighted Binary Cross-Entropy (WBCE) loss function by adding the weight coefficient to measure the importance of different categories based on BCE. The pixel categories hard to learn can be effectively trained by increasing the weight. It can be defined as:

$$\mathcal{L}_{WBCE} = \begin{cases} -\lambda \log(\hat{p}), & y = 1 \\ -(1 - \lambda) \log(1 - \hat{p}), & y = 0 \end{cases}. \quad (2)$$

Focal Loss is a generalized definition of Cross-Entropy (CE) Loss. Lin et al. [20] reduced the loss weight of easily-classified samples by adding an exponential polynomial  $(1 - \hat{p})^\gamma$ , thereby highlighting the loss weight of misclassified samples. This is well known as a good solution of the problem of input imbalance. Its formulation is given as following.

$$\mathcal{L}_{Focal} = \begin{cases} -\lambda(1 - \hat{p})^\gamma \log(\hat{p}), & y = 1 \\ -(1 - \lambda)\hat{p}^\gamma \log(1 - \hat{p}), & y = 0 \end{cases}, \quad (3)$$

where  $\gamma$  represents the hyperparameter used to weight the hard samples. In fact, Focal Loss will degenerate into WBCE Loss when  $\gamma = 0$ . However Focal Loss does not take into account the problem of output imbalance.

### 2.2. Region-based loss

In the region-based loss category, the most basic one is Dice Loss composed of Dice coefficients proposed by Sudre et al. [25]. Dice Loss focuses on the target area, not the background area. Therefore, the gradient of Dice Loss is mainly contributed by the target, whereas the gradient from the background is generally small. Similar to Focal Loss, Dice Loss is suitable for the tasks with serious input imbalance. However, it should also be noted that the mis-classification on the target area has a great impact on Dice Loss and it may even lead to an irreducible loss. In other words, the training of small target using Dice Loss in segmentation is unstable. This shortcoming is fully demonstrated in our experiments: when train networks with our

THC dataset with extreme input imbalance, Dice Loss does not decrease rapidly at the beginning, though its accuracy and segmentation results are better than the distribution-based losses after later convergence. Dice Loss and Dice coefficient are formulated as

$$\mathcal{L}_{Dice} = 1 - D_c, \quad (4)$$

$$D_c = \frac{2TP + \varepsilon}{2TP + FP + FN + \varepsilon}, \quad (5)$$

where  $TP$ ,  $FP$  and  $FN$  refer to the numbers of true positive, false positive and false negative samples respectively.  $\varepsilon$  is used to prevent the denominator from being zero and increase the numerical stability of loss. Generally,  $\varepsilon$  is assigned to 1.

Dice coefficient uses the same weight for FPs and FNs. This is obviously unreasonable in the applications pursuing less  $FP$  more than less  $FN$ . For the imbalance between  $FP$  and  $FN$ , Salehi et al. [15] proposed Tversky coefficient by adding two adjusting parameters  $\alpha$  and  $\beta$  so as to control the output imbalance. Tversky Loss and Tversky coefficient are defined as follows.

$$\mathcal{L}_{Tversky} = 1 - Tv, \quad (6)$$

$$Tv = \frac{TP + \varepsilon}{TP + \alpha FP + \beta FN + \varepsilon}, \quad (7)$$

where  $\alpha$  and  $\beta$  are  $FP$  and  $FN$  regulators respectively. It is noted that when  $\alpha = \beta = 0.5$ , Tversky coefficient degenerates exactly into Dice coefficient.

There is as well a problem with Tversky Loss, that is, no matter what the value of Tversky coefficient ( $Tv$ ) is, its gradient is always constant. It means that when faced with extremely small  $Tv$ , its contribution to the loss is not large, and the loss cannot be reduced efficiently. Inspired by Focal Loss, Abraham et al. [16] propose Focal Tversky (FT) Loss, which can employ  $\gamma$  to highlight the misclassified samples, thus solving the problem of input imbalance. It can be defined as:

$$\mathcal{L}_{FT} = (1 - Tv)^{\frac{1}{\gamma}}, \quad (8)$$

where  $\gamma$  is another hyperparameter used to tune the contribution of hard samples. FT Loss will degenerate into Tversky Loss if  $\gamma = 1$ .

When  $\gamma < 1$ , FT Loss can effectively pay more attention to hard samples, making their loss contribution greater. However, Abraham et al. [16] did not make a more in-depth analysis of its performance on small target segmentation. And the loss change is in fact very small when  $Tv \rightarrow 1$ , leading to over-suppression when the model is close to convergence. They found that  $\gamma = 0.75$  is the best choice.

### 2.3. Compound Loss

Inconsistency between training objectives and inference indexes often leads to poor performance for some indicators. The distribution-based loss is constructed based on the classification accuracy of each pixel, which is more consistent with the indicator of pixel accuracy ( $PA$ ). In contrast, the region-based losses are proposed based on Dice coefficient more consistent with the intersection over union ( $IoU$ ). However,  $IoU$  and  $PA$  are both important indicators in semantic segmentation tasks. In order to make the model perform better in both of them, researchers reported that compound losses are promising by combining distribution-based loss and region-based loss. Combo Loss, Exponential Logarithmic (EL) Loss and Hybrid Focal (HF) Loss belong to this kind.

Combo Loss [10] is a basic compound loss function. It is defined as a convex combination of CE Loss and Dice Loss,

$$\mathcal{L}_{Combo} = \frac{\theta}{wh} \sum_{i=1}^{wh} \mathcal{L}_{WBCE} + (1 - \theta) \mathcal{L}_{Dice}, \quad (9)$$

where  $w$  and  $h$  are the width and height of the image.  $\theta \in (0, 1)$  denotes the tuning hyperparameter of the convex combination.  $\mathcal{L}_{WBCE}$  and  $\mathcal{L}_{Dice}$  are yielded from Eqs. 2, 4 and 5.

The composition form of Exponential Logarithmic (EL) Loss [17] is similar to that of Combo Loss, but the logarithmic exponent is additionally imposed on Dice coefficient and CE. This operation can increase the gradient of small targets in Dice coefficient, and pay more attention to the difficult samples in CE. EL Loss can be defined as:

$$\mathcal{L}_{EL} = \frac{\theta}{wh} \sum_{i=1}^{wh} L_{CE}^{EL} + (1 - \theta) (-\log(D_c))^{\gamma_{D_c}}, \quad (10)$$

where

$$\mathcal{L}_{CE}^{EL} = \begin{cases} \lambda (-\log(\hat{p}))^{\gamma_{CE}}, & y = 1, \\ (1 - \lambda) (-\log(1 - \hat{p}))^{\gamma_{CE}}, & y = 0, \end{cases} \quad (11)$$

and  $D_c$  is Dice coefficient formulated as in Eqs. 4 and 5.  $\gamma_{CE}$  is used to tune the attention of CE part for difficult samples.  $\gamma_{D_c}$  is used to adjust Dice for different input-imbalance levels.

Different from Combo Loss, in order to better adapt to the highly-imbalanced cases, Yeung et al. [18] proposed Hybrid Focal (HF) Loss, replacing CE Loss and Dice Loss with Focal Loss and FT Loss respectively. This is beneficial to the gradient propagation of small targets. HF Loss  $\mathcal{L}_{HF}$  is formulated as:

$$\mathcal{L}_{HF} = \frac{\theta}{wh} \sum_{i=1}^{wh} \mathcal{L}_{Focal} + (1 - \theta) \mathcal{L}_{FT}, \quad (12)$$

where  $\mathcal{L}_{Focal}$  and  $\mathcal{L}_{FT}$  are given in Eqs.3, 8 and 7.

However, HF Loss does not circumvent the inherent shortcomings of Focal Loss and FT Loss, nor does it establish the internal connection between them.

### 3. Proposed Method

#### 3.1. Output imbalance index (OII)

For the class imbalance problem of semantic segmentation, researchers usually take the target to background pixel ratio as an indicator to measure the degree of input imbalance [18]. When studying the output imbalance, this ratio can not manifest the degree of output imbalance intuitively and objectively. Because besides the ratio of  $FP$  to  $FN$ ,  $TP$  is also significant reference. For example, the output imbalance will be almost negligible if  $TP$  is much larger than  $FP$  and  $FN$ . On the contrary, it will have a serious impact on the model performance. And the simple ratio will also shift greatly depending on which one of  $FP$  and  $FN$  is selected as the denominator. For example,  $FP/FN = 0.2$  and  $FN/FP = 5$  show in fact the same degree of output imbalance, but the ratio is totally different.  $FP/FN = 0.2$  and  $FN/FP = 0.2$  denote different degrees of output imbalance, but the ratio is completely the same. This may lead to ambiguity and is not convenient for objective comparison.

In this study we propose a new indicator  $OII$  to measure the degree of output imbalance. Besides,  $OII$  can guide the selection of hyperparameters to adjust the output imbalance.

##### 3.1.1 Formulation and explanation

Not only do  $OII$  considers the values of  $FP$  and  $FN$ , but also considers the  $TP$ . Therefore, it is a function of  $FP$ ,  $FN$  and  $TP$ . The formula is given in Eq.13. For the sake of simplicity, we define variable  $x$  (Eq.14) and attenuation factor  $k$  (Eq.15) as another function of  $FP$ ,  $FN$  and  $TP$ .

$$OII(x) = \begin{cases} 1 - \frac{k}{x + \frac{1}{x} - 1}, & x \in (0, 1], \\ \frac{k}{x + \frac{1}{x} - 1} - 1, & x \in (1, \infty), \end{cases} \quad (13)$$

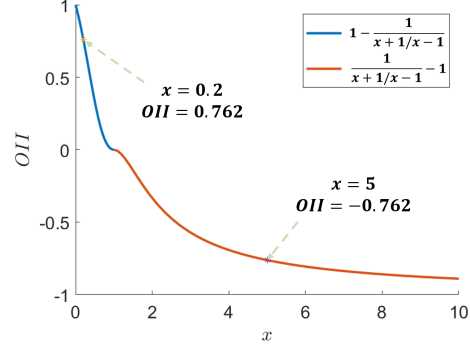
where

$$x = \frac{FP}{FN}, \quad (14)$$

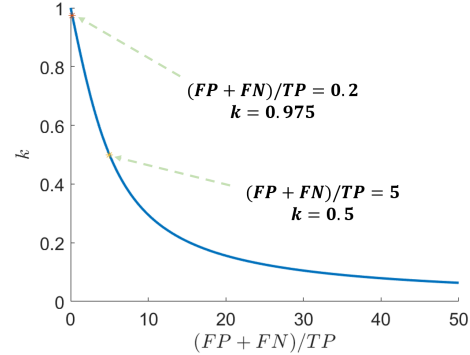
and

$$k = 1 - \frac{2}{\pi} \arctan\left(\frac{FP + FN}{5TP}\right). \quad (15)$$

When  $k \rightarrow 1$ , the change of  $OII$  value with  $x$  is shown in Fig.3a. Obviously,  $OII$  is symmetric with  $FP$  and  $FN$ .  $OII$  result lies in  $(-1, 1)$ . Its algebraic sign shows the case of  $FP > FN$  or  $FP < FN$  and its magnitude denotes the imbalance degree. When the absolute value of  $OII$  is close



(a) The trend of  $OII$  when  $k \rightarrow 1$



(b) Variation of the attenuation factor  $k$

Fig. 3. (a) When  $k \rightarrow 1$ , the change trend of  $OII$  with  $x$  shows that  $OII$  is symmetric with  $x$  and  $1/x$ . (b) The attenuation factor  $k$  changes with the increase of  $(FN + FP)/TP$ .

to 0, the degree of output imbalance is low. Contrarily it is high when the magnitude is close to 1. This new index  $OII$  will facilitate the subsequent research on output imbalance.

When  $TP$  is less than  $FP + FN$ , the output imbalance is nonnegligible. As the value of  $(FP + FN)/TP$  increases, this imbalance needs more attention. Therefore, an attenuation factor  $k \in (0, 1)$  is introduced to further balance the relationship between  $TP$ ,  $FP$  and  $FN$ . When  $FP + FN$  is nearly 5 times of  $TP$ , its  $k$  value approaches to 0.5. The value of  $k$  is defined in Eq.15 and the curve of  $k$  versus  $(FP + FN)/TP$  illustrated in Fig.3b. Clearly, the magnitude of  $OII$  increases monotonously with respect to  $(FP + FN)/TP$ .

For comparison, we employ several representative  $FP$ ,  $FN$  and  $TP$  to evaluate  $FP/FN$ ,  $IoU$ ,  $PA$  and  $OII$  as shown in Table 1. Note from No.1 to No.3,  $OII$  gradually increases with the degree of output imbalance while  $FP/FN$  remains unchanged. From No.3 to No.7,  $(FP + FN)/TP$  is unchanged and  $FP/FN$  changes drastically. At this time,  $IoU$  stays still, while  $OII$  can properly manifest different degrees of imbalance. From No.7 to No.10, it can be found that  $TP/FP$  keeps unchanged and  $FP/FN$  changes greatly,  $PA$  cannot capture the change trend but



Table 1. Using *OII* instead of *FP/FN* to measure output imbalance.

No.	TP:FP:FN	FP/FN	IoU	PA	OII
1	2:0.5:0.5	1	0.667	0.800	0.064
2	2:1:1	1	0.500	0.667	0.126
3	2:3:3	1	0.250	0.400	0.334
4	2:5:1	5	0.250	0.286	-0.844
5	2:4:2	2	0.250	0.333	-0.563
6	2:2:4	0.5	0.250	0.500	0.563
7	2:1:5	0.2	0.250	0.667	0.844
8	2:1:2	0.5	0.400	0.667	0.457
9	2:1:0.5	2	0.571	0.667	-0.397
10	2:1:0.2	5	0.625	0.667	-0.780

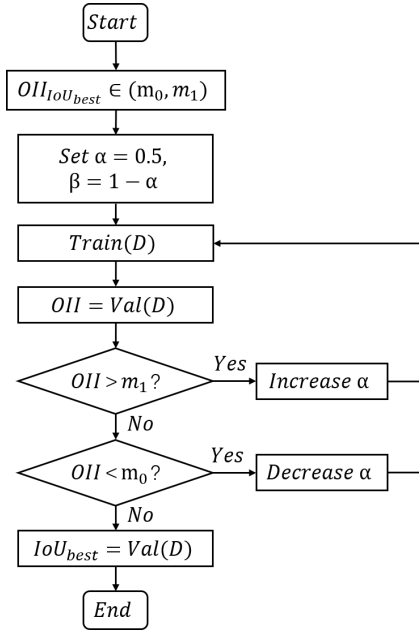


Fig. 4. Use *OII* to guide the selection of  $\alpha$  and  $\beta$ .

*OII* can do. Besides, comparing the pair of No.5 and No.6 as well as the pair of No.4 and No.7, it is noted that *OII* can not only measure the severity of output imbalance in numerical value, but also exactly show the imbalance direction from the algebraic sign.

### 3.1.2 Adaptably guiding hyperparameter selection

*OII* can also be used to guide the selection of hyperparameters  $\alpha$  and  $\beta$  to adjust the output imbalance. The algorithm flow chart shown in Fig.4 finds the best  $\alpha$  and  $\beta$  with the guidance from *OII*.

First, when the *OII* value of the input data  $D$  lies in  $(m_0, m_1)$ , the model performance is better. For example, in this study, we analyze the dataset THC448 in the experi-

ment and found that it can achieve better *IoU* or *PA* when  $OII \in (0.3, 0.4)$ . Next, train a model and use the validating dataset to calculate the *OII* of the model with setting  $\alpha = \beta = 0.5$ . Then readjust the selection of the hyperparameters  $\alpha$  and  $\beta$  with Bisection method by judging the value of the *OII*. For example, in this experiment, if the *OII* is greater than 0.4, increase  $\alpha$  appropriately and train again to get a better *IoU* or *PA*. Finally, by readjusting  $\alpha$  and  $\beta$  several times, the *OII* will fall to the target area  $(m_0, m_1)$  and the model can be greatly improved on *IoU* or *PA*. In order to verify the hyperparameters guidance of *OII*, we put more detailed experimental analysis in Sub-section 4.4.

At present, the most commonly used hyperparameters optimization method is grid search. The superiority of *OII* guidance over grid search is that it greatly saves computational time and improves the efficiency of hyperparameters optimization. In general, we compare the two as follows. If grid search is used to catch the  $\alpha$  in interval  $[a, b]$  which is divided into  $k$  equal part, we set  $\alpha_0 = a$ ,  $\alpha_1 = a + (b-a)/k$ ,  $\alpha_2 = a + 2(b-a)/k$ , ...,  $\alpha_{k-1} = a + (k-1)(b-a)/k$ ,  $\alpha_k = b$  to train  $k+1$  models. If using *OII* guidance to optimise  $\alpha$  in the same interval  $[a, b]$  which then is divided into  $2^n$  equal part, we need to constantly adjust  $\alpha$  with Bisection method to make *OII* fall into the target interval  $(m_0, m_1)$ . It means that we will select  $\alpha_0 = a + (b-a)/2$ ,  $\alpha_1 = a + (b-a)/2^2$ ,  $\alpha_2 = a + (b-a)/2^3$ , ...,  $\alpha_{n-1} = a + (b-a)/2^n$  to train  $n$  models (with  $\alpha$  finally converge to  $a + (b-a)/2^n$  as an example). In fact, when  $\alpha_s = a + (b-a)/2^{s+1}$ , where  $0 \leq s \leq n-1$ , the *OII* may fall into  $(m_0, m_1)$ , so no more than  $n$  models will be trained. In order to fairly compare the complexity of the two hyperparameters optimization methods, we maintain the same refinement of them, dividing interval  $[a, b]$  into  $2^m$  equal part. The length of each subinterval is  $(b-a)/2^m$ . In this case, using grid search for optimization requires training  $2^m + 1$  models. If *OII* guidance is used for optimization, the number of models to be trained should be no more than  $m$ . This means that the optimization efficiency of *OII* guidance is more than  $(2^m + 1)/m$  times that of grid search (e.g., the optimization efficiency of the *OII* guidance is more than 100 times that of grid search when  $n = 10$ ).

### 3.2. Distribution-based DIBE Loss

Although Focal Loss can well adapt to the input imbalance, it can not control the output imbalance. In fact there is no work reporting a distribution-based loss function directly adjusting the output imbalance. [26] and [10] highlighted that the combination of CE Loss and Dice Loss works better than using them individually in many segmentation tasks. The two are based on distribution-based and region-based loss function respectively. Therefore, how to better combine distribution-based loss and region-based loss is a meaning-

ful work. Inspired by the idea of region-based Tversky Loss, in this study we propose a distribution-based loss function, called DIBE<sub>Dis</sub> Loss. By adding *FP* regulator

$\alpha$  and *FN* regulator  $\beta$  to Focal Loss, we enable DIBE<sub>Dis</sub> Loss to adjust the output imbalance. The loss function is formulated as:

$$\mathcal{L}_{DIBE_{Dis}} = \begin{cases} -\lambda(1 - \hat{p})^\gamma \log(\hat{p}), & y = 1, \hat{y} = 1, \\ -\lambda(1 - \hat{p}^{1+\alpha})^\gamma (1 + \alpha) \log(\hat{p}), & y = 1, \hat{y} = 0, \\ -(1 - \lambda)p^\gamma \log(1 - \hat{p}), & y = 0, \hat{y} = 0, \\ -(1 - \lambda)(1 - (1 - \hat{p})^{1+\beta})^\gamma (1 + \beta) \log(1 - \hat{p}), & y = 0, \hat{y} = 1, \end{cases} \quad (16)$$

$$\left. \frac{\partial \mathcal{L}_{DIBE_{Dis}}}{\partial \hat{p}} \right|_{y=1, \hat{y}=0} = \lambda(1 + \alpha)(1 - \hat{p}^{1+\alpha})^\gamma \left( \gamma(1 - \hat{p}^{1+\alpha})^{-1}(1 + \alpha)\hat{p}^\alpha \log(\hat{p}) - \frac{1}{\hat{p}} \right). \quad (17)$$

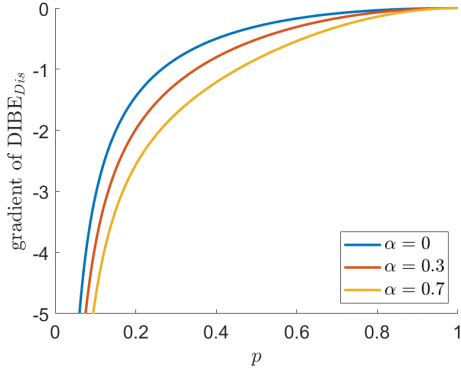


Fig. 5. Gradient curve of DIBE<sub>Dis</sub> under different  $\alpha$ .

where  $\hat{y}$  is predicted label and  $y = 1, \hat{y} = 0$  denotes the regions of *FP*.  $\alpha$  and  $\beta$  are *FP* and *FN* regulator respectively. When  $\alpha = \beta = 0$ , the loss will exactly degenerate into Focal Loss.

To analyze the regulation principle of DIBE<sub>Dis</sub> on output imbalance, the effect of  $\alpha$  (likewise for  $\beta$ ) on output imbalance is taken as an example for analysis. The derivative of DIBE<sub>Dis</sub> Loss at  $y = 1, \hat{y} = 0$  is seen as Eq.17. In order to facilitate comparison and analysis, we fix  $\lambda$  and  $\gamma$  of DIBE<sub>Dis</sub> Loss with 0.25 and 2 respectively, calculate the derivative with  $\alpha \in \{0, 0.3, 0.7\}$  and then get the derivative versus  $\hat{y}$  curve shown in Fig.5. When  $\alpha = 0$ , DIBE<sub>Dis</sub> Loss degenerates into Focal Loss. It can be observed from the figure that the gradient magnitude of DIBE<sub>Dis</sub> is increasing as  $\alpha$  increases. This implies that increasing  $\alpha$  can increase the network's attention to *FP*. In the same way, increasing  $\beta$  can increase the network's attention to *FN*. If  $\alpha = 1 - \beta$  is imposed and  $\alpha \neq \beta$ , the loss gradient of *FP* and *FN* will be different with each other. This difference is the key to control the output imbalance, which is how DIBE<sub>Dis</sub> Loss works. For example, when  $\alpha = 0.3$  and  $\beta = 0.7$ , the loss gradient of  $A_{FN}$  (FN area) is always greater than that of  $A_{FP}$  (FP area). At the moment the loss of  $A_{FN}$  contributes more and the network is more inclined to optimize based on  $A_{FN}$ , making *FN* decrease more strongly than *FP*. Con-

sequently it achieves the purpose of adjusting *FN* and *FP*, leading to  $FN < FP$ .

### 3.3. DIBE Loss

Combo Loss, EL Loss and HF Loss combine the advantages of distribution-based loss and region-based loss. They can not only leverage Dice or Tversky coefficients to deter model parameters from being held at bad local minimum, but also gradually learn better model parameters by decreasing *FP* and *FN* using a cross entropy term. And this combination makes training objectives and inference indexes consistent, finally making the inference performance better. Among them, HF Loss proposed by Yeung et al. [18] is a simple convex combination of Focal Loss and FT Loss, unifying the hyperparameters and demonstrating that HF Loss is better than Focal Loss or FT Loss alone. This allows HF Loss to be used for highly-imbalanced input data, and also to adjust the output imbalance. However, it does not essentially explore the relationship between the two ends.

In this study we proposed DIBE<sub>Dis</sub> Loss in Subsection 3.2 by adding *FP* and *FN* regulators  $\alpha$  and  $\beta$ , so that it can not only work on input imbalance but also harmonise output imbalance. In the region-based loss, we refers to the region-based part of EL Loss and proposes region-based loss for DIBE, named as DIBE<sub>Reg</sub> Loss. DIBE<sub>Reg</sub> Loss can solve the problem that FT Loss will lead to over-suppression of loss then challenge the convergence of model training when  $Tv \rightarrow 1$ . The comparison and gradient analysis of DIBE<sub>Reg</sub> Loss and FT Loss are seen as Appendix A. It is in fact a logarithmic form of Tversky Loss with formula as following:

$$\mathcal{L}_{DIBE_{Reg}} = (-\log(Tv))^{\frac{1}{\gamma}}, \quad (18)$$

where  $Tv$  is Tversky coefficient as defined in Eq.7, and  $\gamma$  is our hyperparameter to specify the level of input imbalance.

Then, a compound loss combining DIBE<sub>Dis</sub> and DIBE<sub>Reg</sub>, namely DIBE Loss, is proposed for extremely-imbalanced input and output. It is in fact a unified form

Table 2. Comparison on datasets selected for experiments.

Dataset	train	val	total	FG:BG	imbalance level
THC448	981	893	1874	1:2228	extreme
THC224	1053	954	2007	1:584	high
THC112	1334	1177	2511	1:191	medium
Blowhole	101	70	171	1:333	high
Crack	46	31	77	1:113	medium
CFD	360	348	708	1:25	low

with clearer parameter meaning as defined below.

$$\mathcal{L}_{DIBE} = \frac{\theta}{wh} \sum_{i=1}^{wh} \mathcal{L}_{DIBEDis} + (1 - \theta) \mathcal{L}_{DIBEReg}, \quad (19)$$

where  $\mathcal{L}_{DIBEDis}$  and  $\mathcal{L}_{DIBEReg}$  are already given in Eqs. 16 and 18.  $\theta, \lambda, \gamma, \alpha, \beta = 1 - \alpha$  in  $\mathcal{L}_{DIBEDis}$  and  $\mathcal{L}_{DIBEReg}$  are the same hyperparameters. Herein,  $\theta$  is used to tune the combining weight of DIBEDis Loss and DIBEReg Loss and we usually set  $\theta = 0.5$ .  $\lambda \in (0, 1)$  is the category weight coefficient controlling the input imbalance. Generally, the selection of  $\lambda$  is based on the ratio of target to background pixels. The smaller the ratio, the closer  $\lambda$  is set to 1 to adapt extreme input imbalance. Given  $\lambda, \gamma$  is the hyperparameter for proper adjustment considering the degree of input imbalance. We set  $\gamma \in [0, 4]$  in our experiments.  $\alpha \in [0, 1]$  is the hyperparameter to control output imbalance. The closer  $\alpha$  is to 1, the stronger the regulation of  $FP$  and the weaker the regulation of  $FN$  are.

## 4. Experiment

### 4.1. Datasets

In this experiment, all the original images of tiny hidden cracks collected were preprocessed to obtain 448×448 input images. Next, defect samples are picked out for labeling and 1874 pairs of input images and labelled images are finally obtained. Some samples are shown in Fig. 6a. 981 pairs of samples are selected as the training dataset, and the remaining 893 pairs of samples are selected as the pixel level validating dataset. In this study, these 1874 pairs of 448×448 samples dataset is named by THC448. Likewise, we built THC224 (1053 pairs in the train set and 954 for the validation set) and THC112 (1334 pairs in the train set and 1177 for the validation set). The essential difference between the three THC datasets is that the degree of input imbalance is gradually alleviated.

The experiments are performed on datasets covering the extremely, highly, medium and low imbalanced cases, i.e. our THC448, THC224, THC112 datasets as well as the public datasets Magnetic Tile Surface Defect Dataset [27]

(MTSDD) and CrackForest Dataset [28] (CFD). See Table 2 for dataset comparison.

The public dataset MTSDD is divided into six sub datasets, also with pixel-level annotations. According to the defect type, they are named respectively Blowhole, Crack, Fray, Break, Uneven and Free (no defects). Dataset CFD contains shadows, oil stains, water stains and other noises samples of urban road surface. Take into account for different levels of imbalance, we select Blowhole, Crack and CFD as well for comparative experiments, see Table 2 for the pixel ratio of target to background. In order to adapt to the input interface of the semantic segmentation model, we further crop and preprocess the samples in Blowhole, Crack and CFD. Some representative samples are shown in Figs. 6d 6e and 6e.

### 4.2. Evaluation metrics

The experiments uses pixel-level performance indicators to evaluate the models and methods. The first selected indicator is the intersection over union ( $IoU$ ) between the prediction and the label. The larger  $IoU$ , the higher the overlap of the region between the prediction and the label, implying the better the semantic segmentation performance. The second indicator is the pixel accuracy ( $PA$ ), measuring the pixel-wise classification accuracy of the semantic segmentation model. The two indicators are defined as follows.

$$IoU = \frac{TP}{TP + FP + FN}, \quad (20)$$

$$PA = \frac{TP}{TP + FP}. \quad (21)$$

### 4.3. Model and configuration

#### 4.3.1 Segmentation model

The experiments mainly employ several classical semantic segmentation models, such as SegNet [29] using the max-pooling index as a skip connection for upsampling, U-Net [30] applying linear interpolation in the process of upsampling, PSPNet [31] using pyramid pooling module to collect levels of information, and DeepLabv3 [32] employing atrous convolution in cascade or in parallel to capture multi-scale context by adopting multiple atrous rates.

#### 4.3.2 Hyperparameters of loss function

In the experiment, for the sake of fairness, we basically follow the optimal hyperparameters mentioned in the original references, and set the same hyperparameters in DIBE Loss. The hyperparameters in all losses are set as:  $\lambda = (0.25, 0.75)$ ,  $\theta = 0.5$ ,  $(\alpha, \beta) = (0.3, 0.7)$ ,  $\gamma_{FT} = 0.75$ ,  $\gamma_{DIBEReg} = 1.5$ ,  $\gamma_{Focal} = \gamma_{DIBEDis} = \gamma_{DIBE} = 2$ ,  $\gamma_{CE} = \gamma_{D_c} = 1$ . In particular, we make a grid search in Table 5 to gain the best hyperparameters  $\lambda, \theta, \alpha$  and  $\gamma$  of



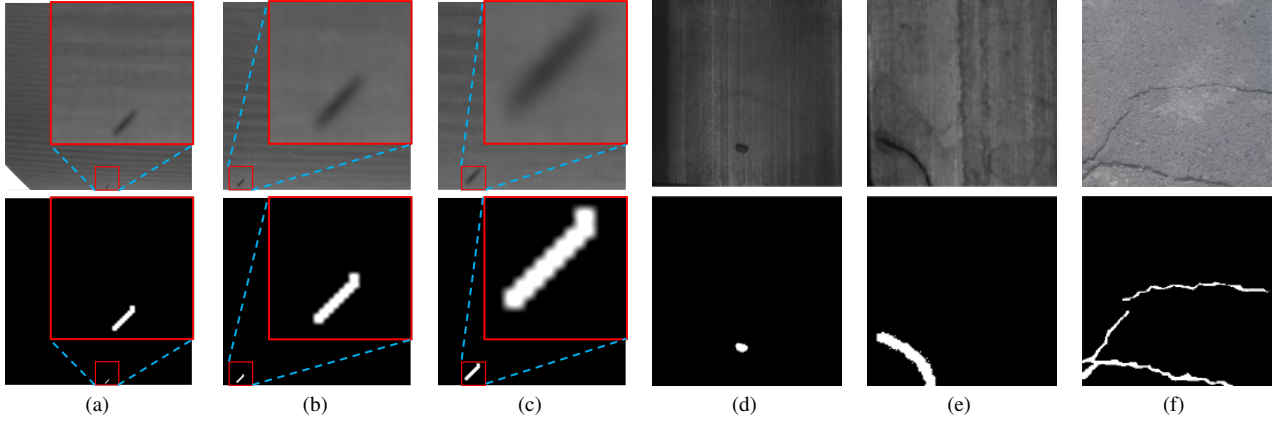


Fig. 6. Sample images of our datasets, MTSDS datasets and CFD dataset. Column (a), (b), (c), (d), (e) and (f) denote pairs of sample images from our THC448, our THC224, our THC112, Blowhole of MTSDS, Crack of MTSDS and CFD respectively. The above of each column is the original image, and the following is the annotation.

each loss. In the experiments in Subsection 4.4 and 4.5, in order to explore how  $DIBE_{Dis}$ ,  $DIBE_{Reg}$  and Tversky Loss harmonise the output imbalance, we only tune the hyperparameters  $\alpha$  and  $\beta$ .

#### 4.3.3 Training configuration

For hardware, a Linux station composed of I7 12700K CPU and two 24G RTX3090Ti GPUs is used in this research for training. Pytorch is used as framework. We use stochastic gradient descent as the optimizer with the initial learning rate 0.01, the momentum 0.9 and batch size 32. The experiments set a fixed random seed, and all training datasets are augmented (flip, contrast, brightness, saturation). The models are trained 50 epochs, and every 5 epochs the validation datasets is tested and  $IoU$ ,  $PA$  and  $OII$  are estimated. All following experiments are performed with the same configuration.

#### 4.4. $OII$ can measure and guide output imbalance

##### 4.4.1 $OII$ can better measure the degree of output imbalance

Using SegNet to train Tversky Loss with THC448 dataset, this study visualizes the curves of  $OII$  and  $FP/FN$  during the training process as shown in Fig. 7. It can be found that the curves of  $FP/FN$  (Fig. 7b) are distributed in  $(0, 25)$  and its upper limit is in fact infinity. This makes it very difficult to measure the change of imbalance in a same scale. For example, when  $\alpha = 0.1, 0.3, 0.5$ , the curves of  $FP/FN$  almost coincide. However, this phenomenon does not exist when the curves of  $OII$  (Fig. 7a) are used to measure the output imbalance. It can be recognized from the chart that  $OII$  values are almost evenly distributed in  $(-1, 1)$ , making the change of imbalance measurable and clearly visible.

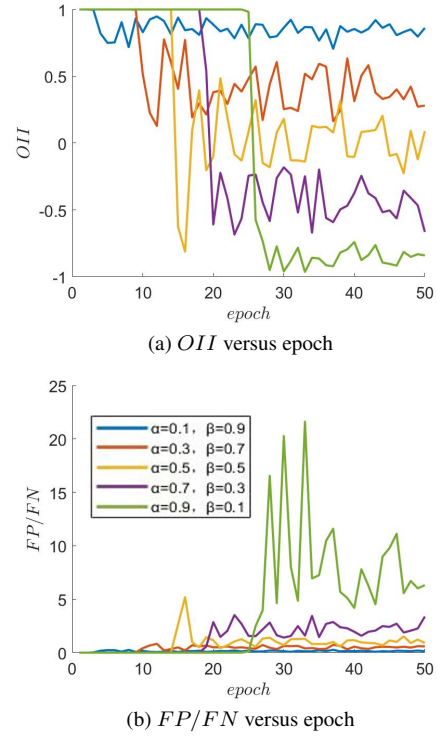


Fig. 7. Comparison between  $OII$  (a) and traditional output imbalance indicator  $FP/FN$  (b) under the same data.

In addition, the relative size relationship between  $FP$  and  $FN$  can also be read from the algebraic sign.

Table 3. Grid Search and *OII* guidance of  $\alpha$  in  $DIB_{Dis}$  Loss and *Tversky* Loss with SegNet and U-Net.

Loss		DIBE <sub>Dis</sub>								Tversky			
	step	$\alpha$	SegNet		$\alpha$	U-Net		$\alpha$	SegNet		$\alpha$	U-Net	
			<i>IoU</i>	<i>PA</i>		<i>IoU</i>	<i>PA</i>		<i>IoU</i>	<i>PA</i>		<i>IoU</i>	<i>PA</i>
Grid Search	1	0.1	<b>0.481</b>	0.823	0.1	0.554	0.843	0.1	0.589	0.891	0.1	0.635	0.863
	2	0.3	0.380	0.646	0.3	0.565	0.851	0.3	0.619	0.830	0.3	0.636	0.798
	3	0.5	0.442	0.713	0.5	0.581	0.832	0.5	<b>0.620</b>	0.774	0.5	<b>0.642</b>	0.782
	4	0.7	0.477	0.709	0.7	<b>0.586</b>	0.800	0.7	0.607	0.725	0.7	0.625	0.724
	5	0.9	0.467	0.657	0.9	0.576	0.785	0.9	0.528	0.581	0.9	0.593	0.671
OII Guidance	1	0.5	0.442	0.713	0.5	0.581	0.832	0.5	0.620	0.774	0.5	0.642	0.782
	2	0.7	<b>0.477</b>	0.709	0.7	<b>0.586</b>	0.800	0.3	0.619	<b>0.830</b>	0.3	0.636	0.798
	3										0.2	0.636	<b>0.840</b>

#### 4.4.2 *OII* can guide the selection of output imbalance hyperparameters

Besides measuring the degree of output imbalance, *OII* can also be used to guide the selection of hyperparameters  $\alpha$  and  $\beta$  to adjust output imbalance. We document the results of *OII* guidance about  $\alpha$  ( $\beta = 1 - \alpha$ ) under Tversky Loss and  $DIB_{Dis}$  Loss in the bottom of Table 3. If the goal of *OII* of THC448 is in the interval of (0.3, 0.4), according to the guidance algorithm in Fig.4 and Bisection method, we use *OII* guidance to select hyperparameter  $\alpha \in [0.1, 0.9]$  and record the steps in the bottom of Table 3. Two guiding examples are explained in Appendix B.

It is recognized that the method of using *OII* to guide the selection of hyperparameters is completely applicable. With the guidance, it is clear to know how to adjust  $\alpha$  and  $\beta$ , rather than enumerating  $\alpha$  and  $\beta$  to select a appropriate value without any reason. Comparing *OII* guidance and grid search in Table 3, it is noted that in most cases, the optimal results found by *OII* guidance are as good as those by grid search with less iterations.

#### 4.5. $DIB_{Dis}$ Loss can adjust output imbalance

The training curves of *OII* in various configurations are demonstrated in Fig.8 and Fig.9. We can find that the adjustment of  $\alpha$  and  $\beta$  of the two losses, i.e.  $DIB_{Dis}$ , Tversky and  $DIB_{Reg}$ , is significant. Regardless of networks and datasets, the *OII* curves locate apart from each other for different  $\alpha$ .

As  $\alpha$  increases from 0.1 to 0.9, the *OII* curves of  $DIB_{Dis}$  Loss are distributed from top to bottom, no matter SegNet or U-Net (Fig.8). And its distributed rule is the same as Tversky Loss, demonstrating the close ability to control the output imbalance for  $DIB_{Dis}$  Loss and Tversky Loss.

As concerning the performance of  $DIB_{Dis}$  Loss in THC112, THC224 and THC448 (left column of Fig.9), it can be found that as the degree of input imbalance increases,

the degree of output imbalance based on distribution-based losses gradually increases (the *OII* curves moves up). Moreover, the ability to control output imbalance also declines with the increase of the input imbalance (the *OII* curves turn to be close to each other). This indicates that input imbalance impacts the result of output imbalance.

Extra usage of  $\alpha$  and  $\beta$  in Focal Loss makes it possible to adjust the output imbalance.  $DIB_{Dis}$  Loss achieved the same output imbalance by tuning  $\alpha$  and  $\beta$  under different input imbalances. For example, in Fig.9 left, the output imbalance of  $\alpha = 0.3$  for THC448 and that of  $\alpha = 0.5$  for THC224 are similar.

#### 4.6. $DIB_{Reg}$ Loss focuses on small target

When *IoU* is constant to 0, we set *OII* to 1. The *OII* curves are always 1 in Figs.8 and 9 refers to that the network is still learning the characteristics of the data and the loss function is difficult to be minimized. Observing the *OII* curves of Tversky in THC112, THC224 and THC448 with U-Net (middle column of Fig.9), it can be found that the higher the degree of input imbalance, the more difficult Tversky Loss is to be minimized.

By comparing the results of using Tversky Loss to train THC112 and using  $DIB_{Reg}$  Loss to train THC448, we found that their *OII* curves are almost the same. It means that after using logarithmic operation,  $DIB_{Reg}$  Loss is more beneficial to the loss minimization of small targets. This is consistent with the analysis in Appendix A. It can also be understood that the process of  $DIB_{Reg}$  Loss minimization for extremely-imbalanced input is similar to that of Tversky Loss minimization for medium/lightly imbalanced input. Therefore,  $DIB_{Reg}$  Loss is more suitable for extremely-imbalanced input data.

To our surprise, by comparing the *OII* curves of  $DIB_{Reg}$  Loss in the datasets THC448, THC224 and THC112 (right column of Fig.9), we found that the *OII* decreases and the curves moves downward as the degree of

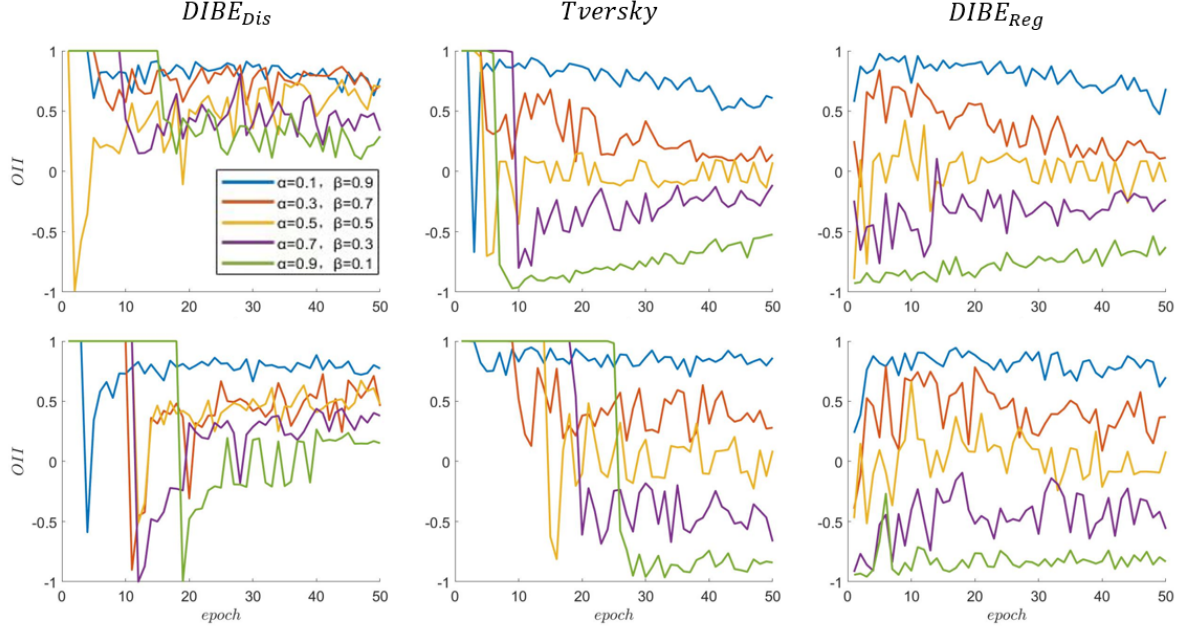


Fig. 8. Regulation of output imbalance of  $\alpha$  in THC448 with different models and different losses. Where the upper row is U-Net and the lower one is SegNet.

input imbalance decreases. According to Fig.3a and Eq.14, if  $OII$  diminishes,  $x$  will scale up and make  $FP$  increasing or  $FN$  decreasing. Therefore, when the degree of input imbalance is low, the logarithmic operation of  $DIBEReg$  Loss focus on minimising  $FN$  rather than minimising  $FP$ .

#### 4.7. DIBE Loss performs better

Due to the proposed  $DIBEReg$  Loss is used to adapt to extremely-imbalanced input data, the experiments in this subsection only compared  $DIBEReg$  Loss to FT Loss, and compared DIBE Loss to HF Loss. First, we trained four networks, i.e. SegNet, U-Net, PSPNet and DeepLabv3 with four loss functions, i.e. FT Loss,  $DIBEReg$  Loss, HF Loss and DIBE Loss respectively. Refer to Section 4.3 for the hyperparameters selected and Table 4 for the training results. It can be found that without any hyperparameters optimization, the results of  $DIBEReg$  Loss and DIBE Loss in THC448 dataset are comparable to or even better than those of FT Loss and HF Loss respectively. And we noted that U-Net has the best segmentation results on dataset THC448 in the four losses.

In order to further compare the segmentation results of DIBE Loss,  $DIBEReg$  Loss, FT Loss and HF Loss, we choose to use datasets with different degree of input imbalance, i.e. THC448, Blowhole, Crack and CFD, to train the four loss functions on U-Net. The grid search is used to do the hyperparameters optimization for the four losses to find the optimal hyperparameters of each loss. We use

the optimal hyperparameters to compare the performance of different losses, and then record the results in Table 5. It is obvious that after fair hyperparameters optimization, DIBE Loss and  $DIBEReg$  Loss we proposed are better than HF Loss and FT Loss in the four datasets. Particularly in THC448 with extreme input imbalance,  $IoU$  obtained significant improvement by  $DIBEReg$  Loss.

Besides better performance,  $DIBEReg$  Loss has the advantage of easier training and earlier convergence than FT Loss. Fig.10 is the result of training U-Net with FT Loss and  $DIBEReg$  Loss on THC448 with optimal hyperparameters. It will be found that in the challenging segmentation task, with the increase of epoch,  $IoU$  is almost zero in the first 20 epochs of the curve of FT Loss in the figure. In other words, FT Loss has the phenomenon of delayed convergence, and in fact requires 30 epochs of training to start to obtain a usable  $IoU$ . By contrast,  $DIBEReg$  Loss can achieve a convincing  $IoU$  at the sixth epoch. The advantage of early convergence of  $DIBEReg$  Loss is very valuable in practical applications, which means that under the same accuracy, it uses half of the computing resources and training time of FT Loss. And its efficiency of training model is twice that of FT Loss, which will be more advantageous in large-scale hyperparameters optimization.

## 5. Discussion

**Why didn't we use cropped image samples so as to get low imbalanced dataset directly?** The background pixels



Fig. 9. Regulation of output imbalance of  $\alpha$  under different input imbalance and different losses. Each row from top to bottom is THC112, THC224, THC448.

Table 4. Results on THC448 with different losses and networks.

Model		SegNet	U-Net	PSPNet	DeepLabv3	Dataset		$FT$	$DIBE_{Reg}$	$HF$	$DIBE$
$FT$	$IoU$	0.607	<b>0.637</b>	0.505	0.539	THC448	$IoU$	0.639	<b>0.652</b>	0.644	<b>0.646</b>
	$PA$	0.811	0.814	0.817	0.919		$PA$	0.823	0.817	0.827	0.817
$DIBE_{Reg}$	$IoU$	0.617	<b>0.637</b>	0.515	0.565	Blowhole	$IoU$	0.774	<b>0.776</b>	0.776	<b>0.779</b>
	$PA$	0.794	0.802	0.792	0.890		$PA$	0.884	0.843	0.851	0.881
$HF$	$IoU$	0.602	<b>0.640</b>	0.547	0.507	Crack	$IoU$	0.708	<b>0.717</b>	0.716	<b>0.723</b>
	$PA$	0.804	0.830	0.796	0.921		$PA$	0.818	0.877	0.889	0.829
$DIBE$	$IoU$	0.600	<b>0.631</b>	0.558	0.519	CFD	$IoU$	0.501	<b>0.510</b>	0.497	<b>0.512</b>
	$PA$	0.791	0.844	0.779	0.932		$PA$	0.821	0.790	0.726	0.880

Table 5. Results of U-Net with different losses and datasets.

can be greatly reduced by cropping the image, thereby alleviating the input imbalance. For example, the THC448, THC224, and THC112 used in the experiment are datasets with gradually reduced input imbalance produced by crop-

ping original images. However, with the increase of cropping degree, the number of inference times increases, leading to a significant computational inefficiency. And it is not applicable in the real scenarios. Therefore, the extremely-



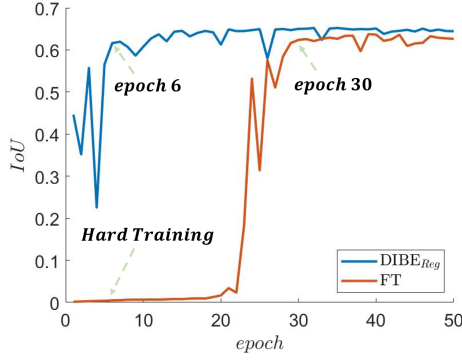


Fig. 10. Training U-Net under FT Loss and  $DIBEReg$  Loss on THC448 with optimal hyperparameters,  $DIBEReg$  has the advantage of early-stop over FT.

imbalanced input is inevitable, and our work provided an alternative way from the loss function.

**Suggestions on the selection of the proposed loss functions.** In the experiment, we found that the training result of  $DIBEReg$  Loss is slightly better than that of DIBE Loss on extremely-imbalanced input dataset. The performance of  $DIBEReg$  Loss, on the contrary, is not as good as that of DIBE Loss on the datasets with medium or high imbalance. Therefore, we recommend using DIBE Loss for the mediumly- and highly-imbalanced cases, and  $DIBEReg$  Loss for the case of extremely-imbalanced input.

**Why  $OII$  can guide the selection of hyperparameters?**  $IoU$  is the most important indicator to measure the performance of the segmentation model. However, for some specific application,  $PA$  also needs to be concerned. According to Eqs. 20 and 21, it can be found that both  $IoU$  and  $PA$  are decided by  $FP$  and  $FN$  which control the output imbalance. Therefore,  $IoU$  and  $PA$  can be improved by using  $OII$  for hyperparameter selection to harmonize the output imbalance.

**DIBE Loss proposed in this work always outperforms HF Loss according to  $IoU$ , but not always according to  $PA$ .** In the hyperparameter optimization, we only used  $IoU$  as the performance index. Thus it is difficult to compare DIBE Loss with HF Loss according to  $PA$ . Using the  $OII$  guidance to adjust  $\alpha$  and fixing other hyperparameters optimized, in our strategy, the  $PA$  can be greatly improved while  $IoU$  value remains unchanged. (see Experiment 4.4.2).

**Two limitations of DIBE Loss.** First, in the adaptive hyperparameter selection for the output imbalance as shown in Fig. 4, the interval  $(m_0, m_1)$  was empirically determined, and also data dependent. Second, the number of hyperparameters both in DIBE loss and HF Loss equals to 4, which is still challenging for specific applications.

## 6. Conclusion and Future work

For the semantic segmentation task with extreme input imbalance, this study proposes three innovative works on both input and output imbalance within the framework of DIBE. Firstly, for the unreasonable indicators to measure the output imbalance, a new measure  $OII$  is introduced to quantify the output imbalance, and an adaptive output imbalance hyperparameter selection method is designed. Secondly, for the distribution-based loss without the ability to adjust the output imbalance, a new distribution-based loss, namely  $DIBEDis$  loss, is provided. Finally, for the inconsistency between training and inference and the lack of loss against extreme input imbalance, DIBE Loss that adapts to extremely-imbalanced input data is proposed. The analysis of loss and its gradient shows the effectiveness of  $DIBEDis$  Loss and DIBE Loss. Extensive experiments validate the effectiveness and efficiency of our method.

In the future, we will firstly further explore the relationship between input imbalance and output imbalance, search for an explicit interval  $(m_0, m_1)$ , and investigate whether the determined interval  $(0.3, 0.4)$  is universal. Secondly, it is useful to study the relationship among hyperparameters in DIBE Loss and then combine some of them with similar functions. Finally, although the  $OII$  and DIBE Loss are built for binary semantic segmentation, they could be easily extended for multi-class tasks, such as detection or classification.

## Acknowledgement

This work was supported in part by Grants of National Key R&D Program of China (No. 2020AAA0108304), in part by the National Nature Science Foundation of China (No. 62171288), and in part by the Shenzhen Science and Technology Program (No. JCYJ20190808143415801).

## References

- [1] H. Zhu, F. Meng, J. Cai, and S. Lu, “Beyond pixels: A comprehensive survey from bottom-up to semantic image segmentation and cosegmentation,” *Journal of Visual Communication & Image Representation*, vol. 34, no. 2, pp. 12–27, 2016.
- [2] C. V. Dung et al., “Autonomous concrete crack detection using deep fully convolutional neural network,” *Automation in Construction*, vol. 99, pp. 52–58, 2019.
- [3] S. Li, X. Zhao, and G. Zhou, “Automatic pixel-level multiple damage detection of concrete structure using fully convolutional network,” *Computer-Aided Civil and Infrastructure Engineering*, vol. 34, no. 7, pp. 616–634, 2019.



- [4] M. H. Hesamian, W. Jia, X. He, and P. Kennedy, "Deep learning techniques for medical image segmentation: achievements and challenges," Journal of digital imaging, vol. 32, no. 4, pp. 582–596, 2019.
- [5] A. Hatamizadeh, Y. Tang, V. Nath, D. Yang, A. Myronenko, B. Landman, H. R. Roth, and D. Xu, "Unetr: Transformers for 3d medical image segmentation," in Proceedings of the IEEE/CVF Winter Conference on Applications of Computer Vision, pp. 574–584, 2022.
- [6] J. Long, E. Shelhamer, and T. Darrell, "Fully convolutional networks for semantic segmentation," in 2015 IEEE Conference on Computer Vision and Pattern Recognition (CVPR), pp. 3431–3440, 2015.
- [7] D. Feng, C. Haase-Schütz, L. Rosenbaum, H. Hertlein, C. Glaeser, F. Timm, W. Wiesbeck, and K. Dietmayer, "Deep multi-modal object detection and semantic segmentation for autonomous driving: Datasets, methods, and challenges," IEEE Transactions on Intelligent Transportation Systems, vol. 22, no. 3, pp. 1341–1360, 2020.
- [8] I. Ulku and E. Akagündüz, "A survey on deep learning-based architectures for semantic segmentation on 2D images," Applied Artificial Intelligence, vol. 36, no. 1, 2022.
- [9] J. M. Johnson and T. M. Khoshgoftaar, "Survey on deep learning with class imbalance," Journal Of Big Data, vol. 6, no. 1, p. 27, 2019.
- [10] S. A. Taghanaki, Y. Zheng, S. K. Zhou, B. Georgescu, P. Sharma, D. Xu, D. Comaniciu, and G. Hamarneh, "Combo loss: Handling input and output imbalance in multi-organ segmentation," Computerized Medical Imaging and Graphics, vol. 75, pp. 24–33, 2019.
- [11] C. Gros, B. De Leener, A. Badji, J. Maranzano, D. Eden, S. M. Dupont, J. Talbott, R. Zhuoquiong, Y. Liu, T. Granberg, et al., "Automatic segmentation of the spinal cord and intramedullary multiple sclerosis lesions with convolutional neural networks," Neuroimage, vol. 184, pp. 901–915, 2019.
- [12] P. F. Christ, M. E. A. Elshaer, F. Ettlinger, S. Tatavarty, M. Bickel, P. Bilic, M. Rempfler, M. Armbruster, F. Hofmann, M. D'Anastasi, et al., "Automatic liver and lesion segmentation in ct using cascaded fully convolutional neural networks and 3d conditional random fields," in International conference on medical image computing and computer-assisted intervention, pp. 415–423, Springer, 2016.
- [13] A. Kannan, A. Hodgson, K. Mulpuri, and R. Garbi, "Leveraging voxel-wise segmentation uncertainty to improve reliability in assessment of paediatric dysplasia of the hip," International Journal of Computer Assisted Radiology and Surgery, vol. 16, no. 7, pp. 1121–1129, 2021.
- [14] M. Qiu, C. Zhang, and Z. Song, "Dynamic boundary-insensitive loss for magnetic resonance medical image segmentation," Medical Physics, vol. 49, no. 3, pp. 1739–1753, 2022.
- [15] S. S. M. Salehi, D. Erdogmus, and A. Gholipour, "Tversky loss function for image segmentation using 3d fully convolutional deep networks," in International workshop on machine learning in medical imaging, pp. 379–387, Springer, 2017.
- [16] N. Abraham and N. M. Khan, "A novel focal tversky loss function with improved attention u-net for lesion segmentation," in 2019 IEEE 16th international symposium on biomedical imaging (ISBI 2019), pp. 683–687, IEEE, 2019.
- [17] K. C. Wong, M. Moradi, H. Tang, and T. Syeda-Mahmood, "3d segmentation with exponential logarithmic loss for highly unbalanced object sizes," in International Conference on Medical Image Computing and Computer-Assisted Intervention, pp. 612–619, Springer, 2018.
- [18] M. Yeung, E. Sala, C.-B. Schönlieb, and L. Rundo, "Unified focal loss: Generalising dice and cross entropy-based losses to handle class imbalanced medical image segmentation," Computerized Medical Imaging and Graphics, vol. 95, p. 102026, 2022.
- [19] X. Li, C. Lv, W. Wang, G. Li, L. Yang, and J. Yang, "Generalized focal loss: Towards efficient representation learning for dense object detection," IEEE Transactions on Pattern Analysis and Machine Intelligence, 2022.
- [20] T.-Y. Lin, P. Goyal, R. Girshick, K. He, and P. Dollár, "Focal loss for dense object detection," in Proceedings of the IEEE international conference on computer vision, pp. 2980–2988, 2017.
- [21] J. Ma, J. Chen, M. Ng, R. Huang, Y. Li, C. Li, X. Yang, and A. L. Martel, "Loss odyssey in medical image segmentation," Medical Image Analysis, vol. 71, p. 102035, 2021.
- [22] S. Jadon, "A survey of loss functions for semantic segmentation," in 2020 IEEE Conference on Computational Intelligence in Bioinformatics and Computational Biology (CIBCB), pp. 1–7, IEEE, 2020.

- [23] M. Yi-de, L. Qing, and Q. Zhi-Bai, "Automated image segmentation using improved pcnn model based on cross-entropy," in Proceedings of 2004 International Symposium on Intelligent Multimedia, Video and Speech Processing, 2004., pp. 743–746, IEEE, 2004.
- [24] V. Pihur, S. Datta, and S. Datta, "Weighted rank aggregation of cluster validation measures: a monte carlo cross-entropy approach," Bioinformatics, vol. 23, no. 13, pp. 1607–1615, 2007.
- [25] C. H. Sudre, W. Li, T. Vercauteren, S. Ourselin, and M. Jorge Cardoso, "Generalised dice overlap as a deep learning loss function for highly unbalanced segmentations," in Deep learning in medical image analysis and multimodal learning for clinical decision support, pp. 240–248, Springer, 2017.
- [26] F. Isensee, P. F. Jäger, S. A. Kohl, J. Petersen, and K. H. Maier-Hein, "Automated design of deep learning methods for biomedical image segmentation," arXiv preprint arXiv:1904.08128, 2019.
- [27] Y. Huang, C. Qiu, and K. Yuan, "Surface defect saliency of magnetic tile," The Visual Computer, vol. 36, no. 1, pp. 85–96, 2020.
- [28] Y. Shi, L. Cui, Z. Qi, F. Meng, and Z. Chen, "Automatic road crack detection using random structured forests," IEEE Transactions on Intelligent Transportation Systems, vol. 17, no. 12, pp. 3434–3445, 2016.
- [29] V. Badrinarayanan, A. Kendall, and R. Cipolla, "Segnet: A deep convolutional encoder-decoder architecture for image segmentation," IEEE transactions on pattern analysis and machine intelligence, vol. 39, no. 12, pp. 2481–2495, 2017.
- [30] O. Ronneberger, P. Fischer, and T. Brox, "U-net: Convolutional networks for biomedical image segmentation," in International Conference on Medical image computing and computer-assisted intervention, pp. 234–241, Springer, 2015.
- [31] H. Zhao, J. Shi, X. Qi, X. Wang, and J. Jia, "Pyramid scene parsing network," in Proceedings of the IEEE conference on computer vision and pattern recognition, pp. 2881–2890, 2017.
- [32] L.-C. Chen, G. Papandreou, F. Schroff, and H. Adam, "Rethinking atrous convolution for semantic image segmentation," arXiv preprint arXiv:1706.05587, 2017.

## Appendix A. Region-based DIBE Loss

Comparing the curve of  $DIBE_{Reg}$  Loss versus  $Tv$  with that of FT Loss versus  $Tv$ , they are shown in Fig.11. It can be found that in the region close to 0,  $DIBE_{Reg}$  Loss is always greater and decreases faster than FT Loss. While  $Tv \rightarrow 1$ ,  $DIBE_{Reg}$  Loss not only has a larger gradient magnitude, but also will not give rise to over-suppression.

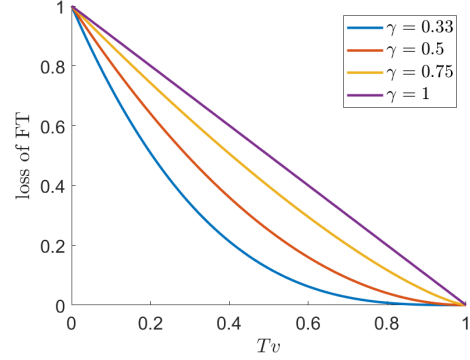
In order to further compare in the scene of extremely-imbalanced input, we take the derivatives of Eqs.8 and 18 respectively as follows.

$$\frac{\partial \mathcal{L}_{FT}}{\partial Tv} = -\frac{1}{\gamma}(1 - Tv)^{\frac{1}{\gamma}-1}, \quad (22)$$

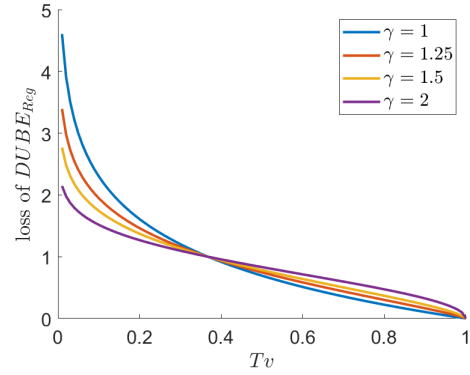
$$\frac{\partial \mathcal{L}_{DIBE_{Reg}}}{\partial Tv} = -\frac{1}{\gamma Tv}(-\log(Tv))^{\frac{1}{\gamma}-1}. \quad (23)$$

The gradients versus  $Tv$  are plotted in Fig.13. By observing Fig.13a, it is found that in the region close to 0, the gradient magnitude of FT Loss is larger than that of Tversky Loss ( $\gamma = 1$  in FT Loss). With the increase of  $Tv$ , however, the gradient magnitude of FT Loss continues to decrease until to zero when  $Tv$  approaches 1. This is exactly the over-suppression phenomenon of FT loss. By contrast, Fig.13b shows that the gradient magnitude of  $DIBE_{Reg}$  Loss is much larger than that of FT Loss in the neighbor of  $Tv = 0$ . As  $Tv$  increases, the gradient magnitude of  $DIBE_{Reg}$  Loss decreases at the beginning and then increases rapidly in the neighbor of 1. This not only settles the problem of over-suppression, but also helps  $DIBE_{Reg}$  Loss focus on small targets segmentation.

In the training phase of network,  $FP$  and  $FN$  are decrease and  $TP$  increases. The degree of input imbalance has a great impact on the relationship of those three. The changes of the three further determine the changes of  $Tv$  (see Eq.6). To study the effect of input imbalance on  $Tv$ , we set  $\alpha = \beta = 0.5$  and treat  $FP$  and  $FN$  as a whole. Considering that the higher the level of input imbalance, the smaller  $TP$  when  $FP$  and  $FN$  are fixed,  $TP$  can thus vary to simulate the change of  $Tv$  in different levels of input imbalance. We use, for example,  $TP = 1, 10, 100$  in Fig.12 respectively to represent the extreme, high and normal level input imbalance. For Fig.12, it can be recognized that with the increase of input imbalance,  $Tv$  will stay close to 0 for a long time during training. Referring to the loss plot (Fig.11) and the gradient plot (Fig.13) of  $DIBE_{Reg}$  Loss, both the loss and gradient magnitude value of  $DIBE_{Reg}$  Loss are larger than that of FT Loss when  $Tv \rightarrow 0$ . Therefore  $DIBE_{Reg}$  Loss has more advantages in dealing with the extremely-imbalanced input data.



(a) Focal Tversky Loss



(b)  $DIBE_{Reg}$  Loss

Fig. 11. (a) Curve of FT Loss changing with Tversky coefficient. (b) Curve of  $DIBE_{Reg}$  Loss changing with Tversky coefficient.

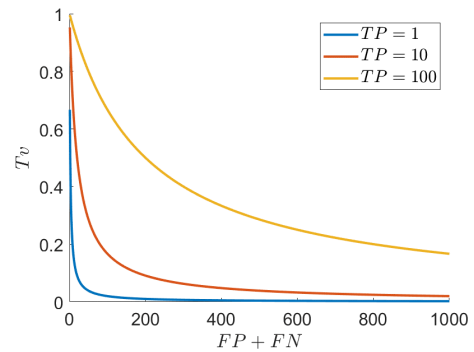
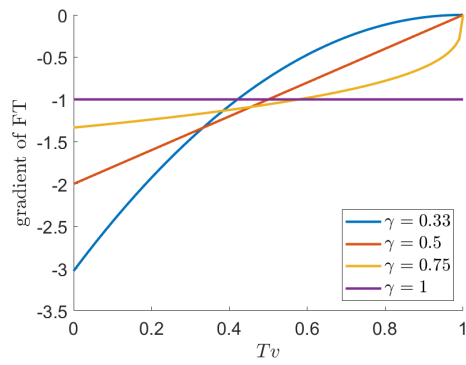
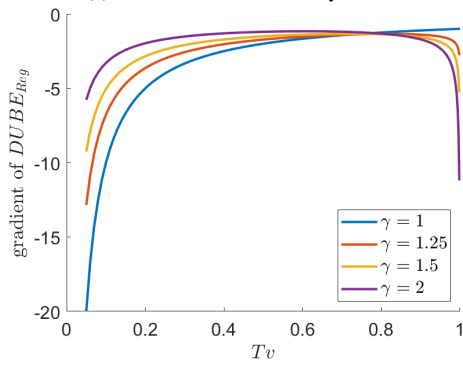


Fig. 12. Curve of  $Tv$  regarding  $TP$ ,  $FP$  and  $FN$ .



(a) Gradient of Focal Tversky Loss



(b) Gradient of  $DIBEReg$  Loss

Fig. 13. Gradients of FT Loss and  $DIBEReg$  Loss versus Tversky coefficient respectively.

## Appendix B. Examples of $OII$ guidance

1. Use  $DIBE_{Dis}$  Loss to train SegNet. At the beginning,  $\alpha_0 = \beta = 0.5$  (centroid of  $[0.1, 0.9]$ ) is set to train the network and yields  $IoU = 0.442$ ,  $PA = 0.713$ ,  $OII = 0.475$ .  $\alpha$  is then increased to reduce  $OII$  because  $OII$  is greater than 0.4 at this time. Then we set  $\alpha_1 = 0.7$  (centroid of  $[\alpha_0, 0.9]$ ) to train the model again and obtain  $IoU = 0.477$ ,  $PA = 0.709$ ,  $OII = 0.322$ . After adjusting  $\alpha$ ,  $OII$  has obviously been decreased to fall into the goal interval  $(0.3, 0.4)$ . Thereby we successfully trade small  $PA$  loss ( $-0.56\%$ ) for greatly improved  $IoU$  ( $+7.92\%$ ).

2. Use Tversky Loss to train U-Net. At the beginning,  $\alpha_0 = \beta = 0.5$  is set to train the network and yields  $IoU = 0.642$ ,  $PA = 0.782$ ,  $OII = 0.071$ .  $\alpha$  is then reduced to increase  $OII$  because  $OII$  is less than 0.3 (centroid of  $[0.1, \alpha_0]$ ) at this time. Then we set  $\alpha_1 = 0.3$  to train the model again and obtain  $IoU = 0.642$ ,  $PA = 0.798$ ,  $OII = 0.118$ . After that,  $OII$  is still less than 0.3, and we continue to decrease  $\alpha$  and set  $\alpha_2 = 0.2$  (centroid of  $[0.1, \alpha_1]$ ) to train the model again and it yields  $IoU = 0.636$ ,  $PA = 0.840$ ,  $OII = 0.382$ . It can be found that  $OII$  is then tuned to fall into the goal interval and  $PA$  has been greatly improved ( $+7.4\%$ ) when  $IoU$  is almost unchanged ( $-1.2\%$ ).